

# Direct shear testing of brittle material samples with non-persistent cracks

Hadi Haeri<sup>\*1</sup>, Vahab Sarfarazi<sup>2</sup>, Alireza Bagher Shemirani<sup>3</sup> and Zheming Zhu<sup>\*\*1</sup>

<sup>1</sup>College of Architecture and Environment, Sichuan University, Chengdu 610065, China

<sup>2</sup>Department of Mining Engineering, Hamedan University of Technology, Hamedan, Iran

<sup>3</sup>Department of Civil, Water and Environmental Engineering, Shahid Beheshti University, Tehran, Iran

(Received August 23, 2017, Revised December 18, 2017, Accepted December 23, 2017)

**Abstract.** The mechanical behavior of the brittle material samples containing the internal and edge cracks are studied under direct shear tests. It is tried to investigate the effects of stress interactions and stress intensity factors at the tips of the pre-existing cracks on the failure mechanism of the bridge areas within these cracks. The direct shear tests are carried out on more than 30 various modeled samples each containing the internal cracks (S models) and edge cracks (E models). The visual inspection and a low power microscope are used to monitor the failure mechanisms of the tested samples. The cracks initiation, propagation and coalescences are being visualized in each test and the detected failure surfaces are used to study and measure the characteristics of each surface. These investigations show that as the ratio of the crack area to the total shear surface increases the shear failure mode changes to that of the tensile. When the bridge areas are fixed, the bridge areas in between the edge cracks have less strength than those of internal cracks. However, the results of this study show that for the case of internal cracks as the bridge area is increased, the strength of the material within the bridge area is decreased. It has been shown that the failure mechanism and fracture pattern of the samples depend on the bridge areas because as the bridge area decreases the interactions between the crack tip stress fields increases.

**Keywords:** bridge area; failure mechanism; crack propagation; direct shear test

## 1. Introduction

The researchers shown that the presence of bridge areas within the natural discontinuity sets play important roles in the stability of rocks and rock-like materials. The most important factors to be considered include the cracks initiation, propagation and coalescence which control the mechanical behavior of such brittle materials. For example, the cracks propagation and coalescence processes may primarily cause the rock mass failures in big rock structures such as slopes, foundations and tunnels.

The pioneered researcher in the crack analysis of brittle material is Griffith (1921) who studied the growth of a pre-existing two-dimensional crack in glass. Since then many works have been performed on the initiation, propagation and coalescence of cracks in brittle materials under various loading conditions. Most of these studies are performed on the cracked specimens which can help to explain the joint (crack) propagation mechanism and serve as useful models for studying the behavior of jointed rock masses and cracked concrete structures (Haeri *et al.* 2014a, b, 2015a, b).

The stiffness of rocks joints in the rock masses may be reduced due to the cracks propagation and coalescence process during the shear failure of rock slopes (Einstein *et*

*al.* 1983). A vast amount of works has been performed on the rock slope stability analyses in the literature (Zhu *et al.* 1997, Grenon and Hadjigeorgiou 2008, Singh *et al.* 2008, Duzgun and Bhasin 2009, Li *et al.* 2009, Gischig *et al.* 2011, Zare Naghadehi *et al.* 2011, Regmi *et al.* 2013, Sharma *et al.* 2013, Akin, 2013, Noël and Soudki 2014, Tiang *et al.* 2015, Wan Ibrahim *et al.* 2015, Li *et al.* 2015, Li *et al.* 2016a, Li *et al.* 2016b, Li *et al.* 2016c, Wang 2016, Li *et al.* 2016d, Li *et al.* 2016e, Wang *et al.* 2017).

The persistence of key discontinuity sets as suggested by Robertson (1970), Einstein *et al.* (1983), may cause the instability of rock slopes because it is more limited and there is a complex interaction in between the already existing natural discontinuities and the brittle fracture propagation in the intact rock bridges. Therefore, the rock bridges may also play an important role in the slope stability due to their effects on the shear strength of the compound failure plane (Einstein *et al.* 1983, Jaeger 1971).

The effects of non-persistent joints (cracks) on the strength of rock masses have been studied by different procedures such as; instrumentations, field observations (as in the Hoek and Brown failure criterion); analytical solutions (as in Jennings's criterion); numerical studies (using available commercial software), or laboratory tests. Among these procedures the laboratory tests may be more attractive because the rock failure mechanism can be exposed where the calibration of the tests may be impossible or very complicated by other means (Haeri 2015a, b, c, Haeri *et al.* 2015c, d, e). The analytical and numerical solutions of many problems in science and engineering are calibrated by laboratory tests.

\*Corresponding author, Professor  
E-mail: [h.haeri@bafgh-iau.ac.ir](mailto:h.haeri@bafgh-iau.ac.ir) or [haerihadi@gmail.com](mailto:haerihadi@gmail.com)

\*\*Corresponding author, Professor  
E-mail: [zhemingzhu@hotmail.com](mailto:zhemingzhu@hotmail.com)

Direct shear tests on the modeled samples containing non-persistent cracks performed by Lajtai (1969). He observed that the failure mode of the model may be changed with increasing the normal stress. He also suggested that a composite failure envelope may be developed to describe the transition from the tensile strength of the intact material to that of the residual strength of the discontinuities. Therefore, the maximum shear strength develops only if the strength of the solid material and that of the cracks are taken into accounts, simultaneously. Further experimental studies carried out to qualitatively visualize the cracks initiations, cracks propagations and cracks coalescences between two or more cracks and, in a qualitative way, the beginning, propagation and coalescence phenomena between two and three cracks (Sagong and Bobet 2002, Mughieda and Alzoubi 2004, Li *et al.* 2005, Mughieda and Khawaldeh 2006, Wang *et al.* 2011, Wang *et al.* 2012, Lancaster *et al.* 2013, Jiang *et al.* 2014, Wang *et al.* 2015, Liu *et al.* 2015, Ning *et al.* 2015, Panaghi *et al.* 2015, Zhao 2015, Yang 2015, Weihua *et al.* 2015). Gehle and Kutter (2003) have shown that the breaking process of the samples and the shear behavior of the intermittent cracks under direct shear loading condition are of most importance in the cracks orientation phenomena which can highly influence the shear strength of the cracked specimens. The shear behavior of rock bridges analyzed by Ghazvinian *et al.* (2007) based on the change in the persistence of their areas. These analyses explained that the failure process and the cracks propagation mechanism may be influenced by the continuity of the bridge area.

The present research investigates the effect of the bridge areas configuration on the shear strength of the non-persistent open cracks. The mechanism of failure process, fracture patterns and shear behavior of the internal and edge cracks under the direct shear testing are thoroughly studied.

## 2. The modeling material and its physical properties

It is seldom possible to perform a full scale testing on a rock mass containing a specified number of cracks with predetermined field configuration. It is important to design the experimental models so that the patterns of discontinuities involved in the field to be preserved in the experimental specimens and the modeling material must behave similar to that of the rock mass. Stimpson (1970) suggested a comprehensive review on the material selection of the modeling samples for rocks. Several researches proposed a number of modeling materials (rock-like materials) to be used instead of the real rocks (Silva *et al.* 2015). Gypsum is one of the mostly used rock-like materials by many researches (Shen *et al.* 1995).

The present research also choose gypsum as the rock-like material because it is an ideal material to model a wide range of brittle materials, behaves as a weak rock and can be casted easily to make several types of experiments (Nelson, 1968). It should be noted that all the previous experiences and results can be incorporated and used so that the earlier findings can be compared with the new ones. However, gypsum allows preparing a large number of specimens and therefore the repeatability of the results is

possible.

The modeled samples may be prepared from a mixture of the water and gypsum with a ratio of water to gypsum as 0.75. The uniaxial compression and indirect tensile tests are concurrently performed with the preparation of specimens and their testing to control the variability of the testing material. Gypsum samples are fabricated in form of cylindrical specimens with 56 mm diameters and 112 mm lengths to measure the uniaxial compressive strength (UCS) of the modeled material. The Brazilian disc type specimens with 56 mm diameters and 28 mm lengths (thicknesses) are also prepared to measure the indirect tensile strength of the material. The ASTM D2938-86 (1986) and ASTM C496-71 (1971), codes are the bases for the testing procedure of the UCS and tensile strength tests, respectively.

In the standard UCS tests, four transducers are used to measure the horizontal and vertical displacements. Three transducers are set longitudinally along a diametrical line at 120 degrees to each other. They touch the middle of the cylindrical specimen longitudinally while the other transducer touches the base of the lower platen of the direct shear test instrument. The transducers and the load cell are connected to a data logger and then linked to a PC for data recording. The UCS and tensile strength of the base material (gypsum) measured from the unconfined compression and indirect tensile tests are as: i) the average uniaxial compressive strength is 40 kg/cm<sup>2</sup>; ii) the average Brazilian tensile strength is 4.5 kg/cm<sup>2</sup>; iii) the average Young's modulus in compression is 6895 MPa and vi) the average Poisson's ratio is 0.14.

## 3. Techniques in preparing the cracked specimens

In general, two main categories of the pre-cracked specimens may be used. In the first category a medium may be inserted in between the two opposing surfaces of the specimen which provides a lower friction angle compared to that of the solid material sample (Stimpson 1970). The second category involves the assembling of the individual small material blocks in a specific shape to form some larger material samples containing persistent joints or non-persistent cracks (Gerges *et al.* 2015). However, fabricating the models of jointed rock masses from the individual rock blocks (elements) may leave some shortcomings such as: the imperfect matching; no closure; no proper fitting of individual elements which leads to the stress concentration in the specimens; block rotations; and non-uniformity of the individual elements (blocks).

These shortcomings caused that Bobet (1997), proposed the sample blocks as a new method to form blocks with the non-persistent open cracks during the samples casting. In this research, the method of preparing samples with the non-persistent open cracks is preferred but some modifications are made to suit the specimens to be fitted in the direct shear test apparatus. It is also tried to prepare pre-cracked specimens with different cracks configurations.

To prepare the required specimens for this study, the material mixture is prepared by mixing water and gypsum in a blender; this mixture is then poured into a specified steel mold. This steel mold of internal dimensions

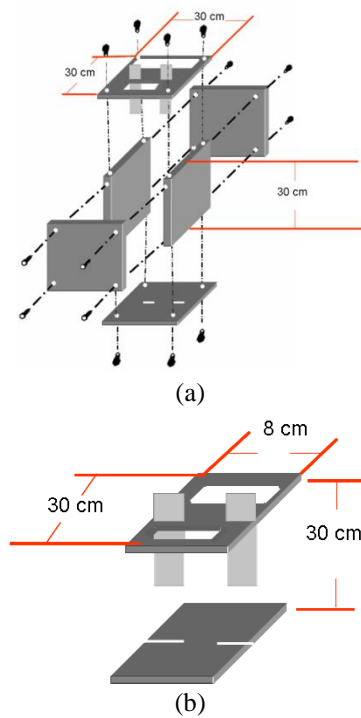


Fig. 1 The modeled samples made from gypsum and used in the direct shear test apparatus, (a) internal cracks configuration and (b) edge cracks configuration

Table 1 Dimension of non-persistent crack

Internal cracks				Edge cracks			
2a (cm)	b (cm)	2a (cm)	b (cm)	2a (cm)	b (cm)	2a (cm)	b (cm)
3	2	3	4	3	6	3	2
2.5	2	2.5	4	2.5	6	2.5	3
2	2	2	4	2	6	2	4
1.5	2	1.5	4	1.5	6	1.5	5
1	2	1	4	1	6	1	6
3	3	3	5				
2.5	3	2.5	5				
2	3	2	5				
1.5	3	1.5	5				
1	3	1	5				

30×30×30 cm is modified to prepare the specific pre-cracked modeled specimens containing the internal cracks (S cracked model). Another steel mold is designed with the internal dimension of 30×8×30 cm which can be used to prepare the modeled samples with the specified edge cracks (E cracked model). These two modeling configurations are shown in Fig. 1(a) and 1(b), respectively.

Fig. 1 shows that these steel molds are made of four steel sheets (bolted together) and of two PMMA plates 1/6-

inch-thick, which are placed at the top and bottom of the mold. The top plates contain two rectangular openings for filling the steel mold with the liquid gypsum mixture. There are some slits (cuts) in the upper and the lower surfaces of the mold. The apertures of these slits are 0.5 mm (0.02 inch) and their lengths (persistence) changes based on the width of the cracks. Before pouring the gypsum into the mold, the greased metallic shims are inserted into these slits which are passing through the thickness of the steel mold to produce the open cracks within the modeled samples. The fresh gypsum is vibrated within the mold and then stored at room temperature for 8 hours. The casted specimens are then unmolded and the metallic shims are pulled out of the specimens. It should be noted that the polished grease on the shims prevents them to adhere with the gypsum and therefore facilitates their removal from the specimens. It does not the shim removal produces any damage to the flaws. On the other hand, a number of pairs of PMMA plates are prepared (with different slit arrangements) to produce the desired crack geometries. The shims leave corresponding open cracks through the thickness of the specimens which are at right angles to the front and back of these specimens as the gypsum seated and hardened in the laboratory room. The front and back of the specimens are polished immediately after the shims removal and stored in the lab for 4 days to be cured and then be ready for the direct shear tests. The bridge areas within these modeled samples varies from 60 cm<sup>2</sup> to 180 cm<sup>2</sup> with increments of 30 cm<sup>2</sup> while in the fixed areas of the bridges, the cracks areas vary from 60 cm<sup>2</sup> to 360 cm<sup>2</sup> (with the increments of 60 cm<sup>2</sup>). The bridge areas in the models vary from 60 cm<sup>2</sup> to 180 cm<sup>2</sup> (with the increments of 30 cm<sup>2</sup>). Table 1 show the geometry of non-persistent cracks. The bridge area dimensions are defined by parameter b and the crack dimensions are defined by parameter 2a in the figures shown in this table.

The complete failure behavior in the discontinuities, from each geometry and material strength are studied by preparing three similar blocks specimens and testing them in a direct shear test apparatus under three different normal stresses ( $\sigma_n$ ): 3.33, 5.55 and 7.77 kg cm<sup>-2</sup>. Two similar specimens are prepared for each normal loading and then tested to check the repeatability of the results. However if there is a significant difference in between the results obtained from these two identical tests then a third specimen is prepared and tested to find a closer results of the shear failure behavior of the pre-cracked specimens.

#### 4. The proposed testing equipment

The direct shear testing of the specimens are continued till their final failure is reached and a specially designed direct shear testing apparatus is used to perform these experiments in the laboratory. Therefore, the two high stiffness shear boxes with only one degree of freedom for each box (in the horizontal direction for the lower box and in the vertical direction for the upper box) are designed to measure both shear displacement (horizontal displacement) and dilation simultaneously. This robust configuration prevents the unwanted rotations and uncontrolled loading

conditions in the testing apparatus. In order to permanently visualize the fracturing process in the sheared specimens, the arrangements of the shear boxes are appropriately established to permit some free faces in front and back sides of the specimens. However, the direct shear testing of 180 specially modeled specimens is performed and their failure process is investigated in the laboratory. All of these tests are displacement-controlled and can be performed in such a way that a constant normal load is applied to the sample and then the shear load is incrementally increased till the specimen fails. Every two seconds the shear loads and the corresponding shear displacements are recorded by a data acquisition system. A displacement control rate of 0.002 mm/s is used during the experiments testing. However, the basic measurements are the failure mode, the fracture patterns and the failure and cracks coalescence stresses.

**5. Experimental observations of the fracture patterns in the modeled samples**

The variation of the fracture pattern base on the ratio of crack surface to the total shear surface is studied by observing the fracture surface during and after the tests. The failure mechanism of the tested samples is influenced by the normal load and the ratio of crack surface to total shear surface. For example, the fracture patterns in two different tested samples containing internal and edge cracks is shown in Fig. 2.

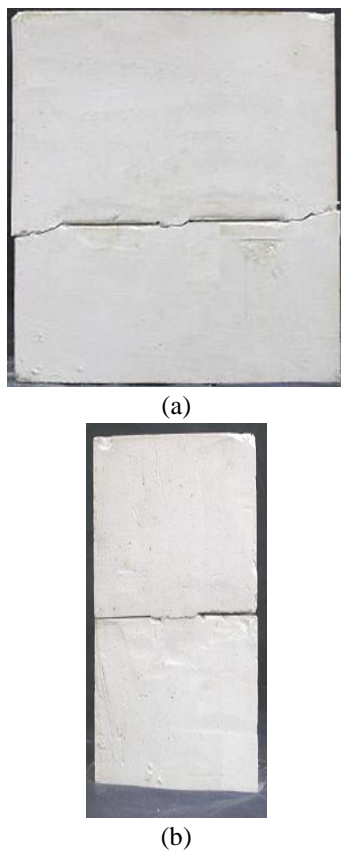


Fig. 2 Fracture patterns in the tested samples consisting (a) internal cracks and (b) edge cracks

Non-persistent crack set		The Failure patterns in bridge areas		
Edge cracks				
Internal cracks				

Fig. 3 The fracture patterns in bridge areas of the tested samples

All of the observed cracks patterns obtained from the direct shear tests on the modeled samples are summarized in Fig. 3. Two types of crack propagation mechanisms are observed known as; wing (tensile) cracks and shear (secondary) cracks. The wing cracks generally start from the crack tips and as the loading is in progress they propagate in a curvilinear path till coalesce with each other, with the nearby cracks or meet the specimen's borders. The wing cracks are also known as tensile cracks grow in a stable manner starting their initiations and propagations first due to the lower tensile strengths of the modeled samples but the shear cracks also known as the secondary cracks may initiate at the crack tips and may propagate in a stable or unstable manner.

**5.1 The oval mode of cracks coalescence with two wing cracks**

Fig. 3(a) and 3(b) show that the oval mode of cracks coalescence occurs in the tested samples with edge or internal cracks under 3 normal loads, for the case  $(4a/(4a+b)) > 0.55$ . In these samples the wing cracks are initiated and propagated in curvilinear paths and eventually get aligned with the direction of shear loading. These cracks propagate in a stable manner and for further propagation the external load needs to be increased. It can be easily observed that each wing crack is initiated at the tip of one crack and continue its propagation till get coalesced with the tip of the other crack. A relatively similar results gained by Zhang, (2006) showing that the oval mode of cracks coalescence occurs in a critical range of crack separation  $(0.9 \leq b/4a \leq 1.25)$  by direct shear testing on the modeled samples of plaster.

**5.2 The cracks coalescence with one convex wing crack**

This mode of cracks coalescence (as shown in Fig. 3(b) and 3(e)) occurs in the edge or internal cracks under three loads for the case  $0.375 < (4a/(4a+b)) \leq 0.55$ . In this mode, the wing cracks are getting initiated at the cracks tips and then extended in a stable manner. The upper convex crack may extend into the intact part of the samples and finally coalesce with the inner tip of the other crack. The lower tensile (wing) crack may develop and propagate to a relatively far distance from the crack tip and then getting

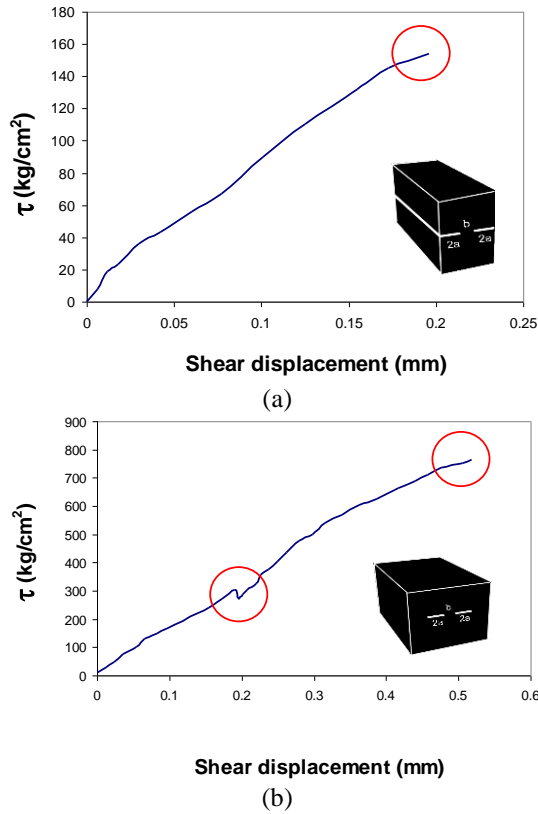


Fig. 4 The shear stress-shear displacement curves ( $\tau$ - $u$ ) for specimens consisting (a) edge cracks and (b) internal cracks

stable so that it may not coalesce with the tip of opposite crack. It may be noticed that there is a smooth and clean wing crack surface with no crushed or pulverized material on it therefore, there is no evidence of shear displacement or shear cracking surface. Therefore, this crack surface examination shows that the crack surface characteristics are indicator of the tensile stresses which are responsible for the initiation and propagation of the wing cracks. However, in this mode, the normal loads are low enough to allow the tensile (wing) cracks production.

**6. The shear mode cracks coalescence**

This mode of cracks coalescence is known as the shear mode and is shown in Fig. 3(c) and 3(f). This kind of cracks coalescence mainly occurs in tested samples with the edge or internal cracks under three normal loads when  $0.25 < (4a/(4a+b)) \leq 0.375$ . In the shear mode, the wing cracks are mainly getting initiated at the cracks tips and then propagating in a stable manner within the tested specimens. The main characteristic of the failure mechanism of the samples is that the initiation of wing cracks is followed by the initiation of secondary (shear) cracks at the cracks tips. Therefore, the two stable wing cracks may get arrested while the two secondary cracks continue their extension till coalesce at a point in the bridge area in between the two inner tips of the preexisting cracks. However, the bridge area may be failed due to the propagations and coalescences of the secondary cracks within the tested samples.

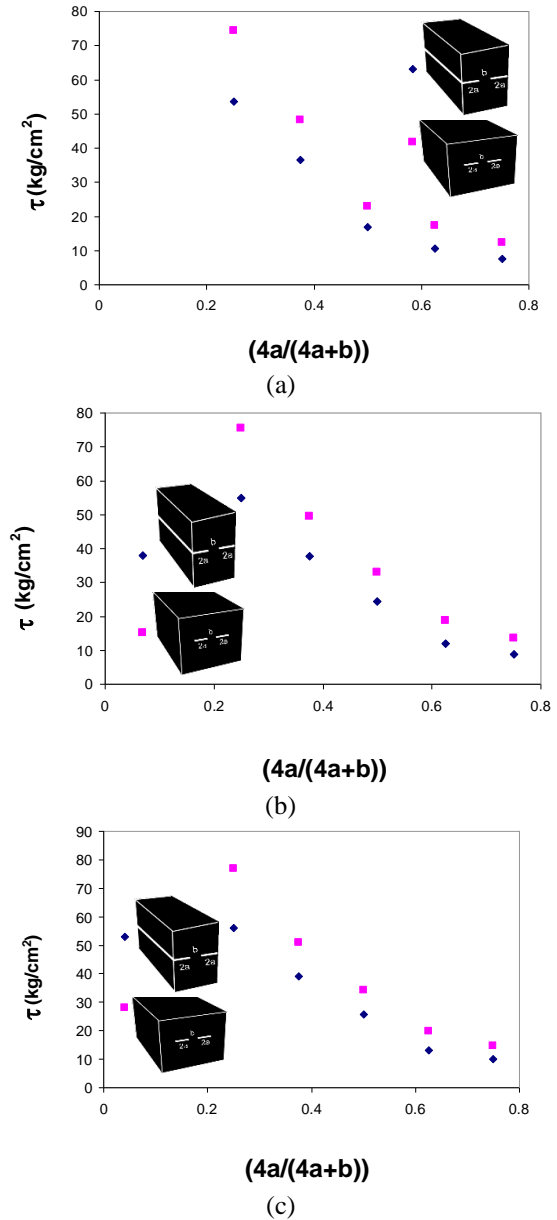


Fig. 5 The rock-bridge strengths versus the increasing values of  $(4a/(4a+b))$  for (a)  $\sigma_n=3.33 \text{ kg/cm}^2$ , (b)  $\sigma_n=5.55 \text{ kg/cm}^2$  and (c)  $\sigma_n=7.77 \text{ kg/cm}^2$

Observation of the crack surfaces show that the shear failure surface is in a wavy form. Further inspection of the cracks surfaces produced by coalescence may reveals many small kink steps, crushed gypsum and gypsum powder on these surfaces therefore, it may be concluded that the cracks coalescence phenomena is due to shearing in this mode.

**6.1 Shear stress-shear displacement curves for samples with edge and internal cracks**

The curves of shear stress-shear displacement ( $\tau$ - $u$ ) for the specimens with edge and internal cracks are shown in Fig. 4(a) and 4(b), respectively. The curve in Fig. 4(a) shows one downfall portion for the bridge area failure for the edge cracked specimen but there are two such downfalls in Fig. 4(b) for the specimen with two internal cracks. In

Fig. 4(b), the first and the second downfalls represent the bridge area failure and the final stage of failure in this specimen, respectively. The first downfalls in Fig. 4(b) shows the failure of rock bridge situated between the joint.

All of the tested samples show the same behavior therefore, the strength of the bridge area can be measured from these curves for further analysis.

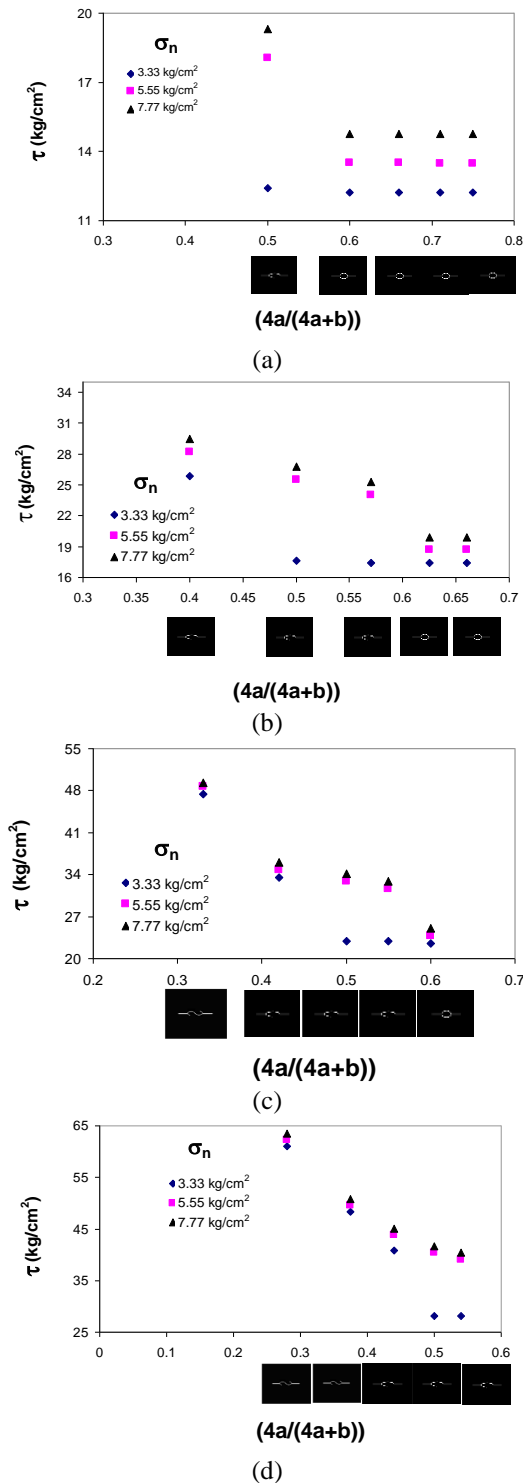


Fig. 6 The rock-bridge strengths versus the increasing values of  $(4a/(4a+b))$  ratio for (a)  $b=60 \text{ cm}^2$ , (b)  $b=90 \text{ cm}^2$ , (c)  $b=120 \text{ cm}^2$ , (d)  $b=150 \text{ cm}^2$  and (e)  $b=180 \text{ cm}^2$ , respectively

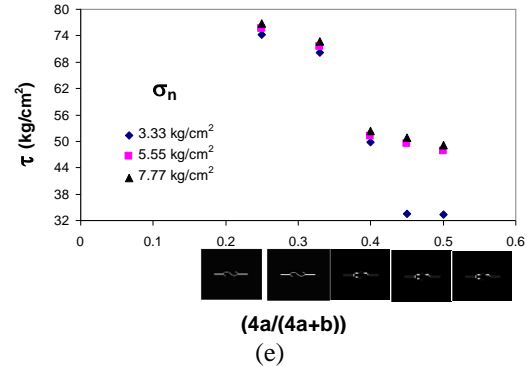


Fig. 6 Continued

### 6.2 Effects of the ratio of crack surface to the total shear surface

It has been shown that for the case  $(4a/(4a+b)) > 0.55$ , no new fracture (crack) is produced in the midst zone of the sample due to the high stress interactions in between the cracks therefore, the oval mode shown in Fig. 2(a) and 2(b) may appear. On the other hand, when  $0.375 < (4a/(4a+b)) \leq 0.55$ , the stress interaction in between cracks is low so that the cracks coalescence with one convex wing crack may occur in bridge area of the sample similar to that shown in Fig. 2(b) and 2(e). In this case, in fact, the interaction in between the cracks is not so enough to result in the oval mode cracks coalescence. However, when  $0.25 < (4a/(4a+b)) \leq 0.375$ , there is not any stress interaction in between the cracks so that the cracks coalescence mode is that of the shear one which may occur in bridge area of the samples (Fig. 2(c) and 2(f)). Therefore, it may be clear that by decreasing the value of  $(4a/(4a+b))$ , the stress interaction in between the cracks may decrease so that the shear mode of fracture produces in the midst zone of the tested samples.

### 6.3 Comparing the bridge area strengths of the edge and internal cracked samples

The bridge area strengths versus the increasing values of  $(4a/(4a+b))$  ratio are depicted in Fig. 5(a)-5(c), for the normal loads of  $3.33 \text{ kg/cm}^2$ ,  $5.55 \text{ kg/cm}^2$  and  $7.77 \text{ kg/cm}^2$ , respectively. The upper and the lower lines in each panel illustrate the bridge area strengths in between the surrounding cracks and those of the edge cracks, respectively.

The results shown in Fig. 5(a)-5(c) show that the bridge area strengths in between the internal cracks is higher than those for the edge cracks when the fixed values of  $(4a/(4a+b))$  are considered. Fracture mechanics principles predict the same results because the mode I and Mode II stress intensity factors (KI and KII) of the internal cracks in the tested samples are comparatively lower than those of the samples with the edge cracks (at equal cracks length) which leads to a higher bridge area strength of the samples with internal cracks.

### 6.4 Effects of the ratio of internal crack surface to total shear surface

The rock bridge strength versus the increasing values of

the  $(4a/(4a+b))$  is shown in Fig. 6. The failure process of the cracked specimens considering the three different normal stresses are shown in this figure. Fig. 6(a)-6(f) shows the bridge area strengths for the bridge areas of  $60 \text{ cm}^2$ ,  $90 \text{ cm}^2$ ,  $120 \text{ cm}^2$ ,  $150 \text{ cm}^2$  and  $180 \text{ cm}^2$ , respectively.

It may be concluded that the bridge area strength decrease dramatically by increasing the ratios of  $(4a/(4a+b))$  (i.e. increasing the internal cracks areas) for the case of a fixed bridge area and under a fixed normal stress condition. However, as the planar wing cracks coalescence change to that of the oval mode the bridge area strength may highly decrease which is due to increasing in the stress intensity factors at the crack tips and in the stress interaction between the cracks. The bridge area strengths may become constant, for the fixed bridge areas in the case of  $(4a/(4a+b)) > 0.6$  ratio (as shown in Fig. 1(a) and 1(b)). Therefore, increasing in the crack surface areas may not affect the bridge area strengths of the tested samples for  $(4a/(4a+b)) > 0.6$  ratio because the interaction in between the cracks is so strong with in the specimens.

## 7. Conclusions

The shear behavior of the relatively weak rock specimens containing non-persistent internal and edge cracks with different bridge areas have been studied for the direct shear tests under three different normal loads. These experimental tests may result in the following conclusions:

I) The wing cracks combination may be produced in the fracture patterns with in the samples under low values of normal loads.

II) The oval mode of cracks coalescence with two wing cracks occur in the samples with edge or internal cracks when  $(4a/(4a+b)) > 0.6$ . This is due to the high stress interactions in between the cracks where no new fracture surfaces produce in the midst zone of the tested specimens.

III) The crack coalescence mode with one convex wing crack may occur in the samples containing edge or internal cracks when  $0.375 < (4a/(4a+b)) \leq 0.6$  because the low stress interactions in between the cracks in the tested specimens.

IV) There may not be any stress interaction in between the cracks within the samples containing the edge and internal cracks when  $0.25 < (4a/(4a+b)) \leq 0.375$ , therefore, the cracks coalescence mode with one planar wing crack may occurs in the tested samples.

V) The bridge area strengths in between the internal cracks of the tested samples is usually higher than those of the samples with edge cracks when the values of  $(4a/(4a+b))$  are fixed.

VI) The bridge area strengths in between the internal cracks of the tested samples are decreasing dramatically due to increasing the ratio of  $(4a/(4a+b))$  for a fixed bridge area and under a fixed normal loading condition but the bridge area strength becomes constant for the ratio of  $(4a/(4a+b)) > 0.6$ .

## References

Akin M. (2013), "Slope stability problems and back analysis in

- heavily jointed rock mass: A case study from Manisa, Turkey", *Rock Mech. Rock Eng.*, **46**(2), 359-371.
- ASTM, (1971), *Standard Method of Test for Splitting Tensile Resistance of Cylindrical Concrete Specimens*, ASTM Designation C496-71.
- ASTM, (1986), *Test Method for Unconfined Compressive Resistance of Intact Rock Core Specimens*, ASTM Designation D2938-86.
- Bobet, A. (1997), "Fracture coalescence in rock materials: Experimental observations and numerical predictions", Sc.D. Dissertation, Massachusetts Institute of Technology, Cambridge, U.S.A.
- Duzgun, H.S.B. and Bhasin, R.K. (2009), "Probabilistic stability evaluation of Oppstadhornet rock slope, Norway", *Rock Mech. Rock Eng.*, **42**(5), 729-749
- Einstein, H.H., Veneziano, D., Baecher, G.B. and O'Reilly, K.J. (1983), "The effect of discontinuity persistence on rock stability", *J. Rock Mech. Min. Sci. Geomech. Abstr.*, **20**(5), 227-236.
- Gehle, C. and Kutter, H.K. (2003), "Breakage and shear behavior of intermittent rock joints", *J. Rock Mech. Min. Sci.*, **40**(5), 687-700.
- Gerges, N.N., Issa, C.A. and Fawaz, S. (2015), "Effect of construction joints on the splitting tensile strength of concrete", *Case Stud. Construct. Mater.*, **3**, 83-91.
- Ghazvinian, A., Nikudel, M.R. and Sarfarazi, V. (2007), "Effect of rock bridge continuity and area on shear behavior of joints", *Proceedings of the 11<sup>th</sup> Congress of the International Society for Rock Mechanics*, Lisbon, Portugal, July.
- Gischig, V., Amann, F., Moore, J.R., Loew, S., Eisenbeiss, H. and Stempfhuber, W. (2011), "Composite rock slope kinematics at the current Randa instability, Switzerland, based on remote sensing and numerical modeling", *Eng. Geol.*, **118**(1-2), 37-53.
- Grenon, M. and Hadjigeorgiou, J. (2008), "A design methodology for rock slopes susceptible to wedge failure using fracture system modeling", *Eng. Geol.*, **96**(1-2), 78-93.
- Griffith, A.A. (1921), "The phenomena of rupture and flow in solids", *Philos. Trans. R. Soc. London Ser. A*, **221**(582-593), 163-198.
- Haeri, H., Shahriar, K. and Marji, M.F. (2013), "Modeling the propagation mechanism of two random micro cracks in rock samples under uniform tensile loading", *Proceedings of the 13<sup>th</sup> International Conference on Fracture*, Beijing, China, June.
- Haeri, H., Shahriar, K., Marji, M.F. and Moarefvand, P. (2014a), "On the cracks coalescence mechanism and cracks propagation paths in rock-like specimens containing pre-existing random cracks under compression", *J. Centr. South Univ.*, **21**(6), 2404-2414.
- Haeri, H., Shahriar, K., Marji, M.F. and Moarefvand, P. (2014b), "Investigating the fracturing process of rock-like Brazilian discs containing three parallel cracks under compressive line loading", *Strength Mater.*, **46**(3), 133-148.
- Haeri, H. (2015a), "Propagation mechanism of neighboring cracks in rock-like cylindrical specimens under uniaxial compression", *J. Min. Sci.*, **51**(3), 487-496.
- Haeri, H. (2015b), "Influence of the inclined edge notches on the shear-fracture behavior in edge-notched beam specimens", *Comput. Concrete*, **16**(4), 605-623.
- Haeri, H. (2015c), "Simulating the crack propagation mechanism of pre-cracked concrete specimens under shear loading conditions", *Strength Mater.*, **47**(4), 618-632.
- Haeri, H., Khaloo, A. and Marji, M.F. (2015a) "Fracture analyses of different pre-holed concrete specimens under compression", *Acta Mech. Sin.*, **31**(6), 855-870.
- Haeri, H., Shahriar, K., Marji, M.F. and Moarefvand, P. (2015b), "On the HDD analysis of micro cracks initiation, propagation and coalescence in brittle substances", *Arab. J. Geosci.*, **8**(5),

- 2841-2852.
- Haeri, H., Marji, M.F. and Shahriar, K. (2015c), "Simulating the effect of disc erosion in TBM disc cutters by a semi-infinite DDM", *Arab. J. Geosci.*, **8**(6), 3915-3927.
- Haeri, H., Khaloo, A. and Marji, M.F. (2015d), "Experimental and numerical simulation of the microcracks coalescence mechanism in rock-like materials", *Strength Mater.*, **47**(5), 740-754.
- Haeri, H., Khaloo, A. and Marji, M.F. (2015e), "Experimental and numerical analysis of Brazilian discs with multiple parallel cracks", *Arab. J. Geosci.*, **8**(8), 5897-5908.
- Ibrahim, M.W., Hamzah, A.F., Jamaluddin, N., Ramadhansyah, P.J. and Fadzil, A.M. (2015), "Split tensile strength on self-compacting concrete containing coal bottom ash", *Proc. Soc. Behav. Sci.*, **198**, 2280-2289.
- Jaeger, J.C. (1971), "Friction of rocks and stability of rock slopes", *Geotechnique*, **21**(2), 97-134.
- Jiang, Z., Wan, S., Zhong, Z., Li, M. and Shen, K. (2014), "Determination of mode-I fracture toughness and non-uniformity for GFRP double cantilever beam specimens with an adhesive layer", *Eng. Fract. Mech.*, **128**, 139-156.
- Lajtai, E.Z. (1969), "Resistance of discontinuous rocks in direct shear", *Geotechnique*, **19**, 218-233.
- Lancaster, I.M., Khalid, H.A. and Kougioumtzoglou, I.A. (2013), "Extended FEM modelling of crack propagation using the semi-circular bending test", *Construct. Build. Mater.*, **48**, 270-277.
- Li, D., Zhou, C., Lu, W. and Jiang, Q. (2009), "A system reliability approach for evaluating stability of rock wedges with correlated failure modes", *Comput. Geotech.*, **36**(8), 1298-1307.
- Li, S., Wang, H., Li, Y., Li, Q., Zhang, B. and Zhu, H. (2016), "A new mini-grating absolute displacement measuring system for static and dynamic geomechanical model tests", *Measurement*, **105**, 25-33.
- Li, Y., Li, C., Zhang, L., Zhu, W., Li, S. and Liu, J. (2016), "An experimental investigation on mechanical property and anchorage effect of bolted jointed rock mass", *Geosci. J.*, **21**(2), 253-265.
- Li, Y., Zhou, H., Zhu, W., Li, S. and Liu, J. (2016), "Experimental and numerical investigations on the shear behavior of a jointed rock mass", *Geosci. J.*, **20**(3), 371-379.
- Li, Y., Zhou, H., Zhu, W., Li, S. and Liu, J. (2015), "Numerical study on crack propagation in brittle jointed rock mass influenced by fracture water pressure", *Materials*, **8**(6), 3364-3376.
- Li, Y.P., Chen, L.Z. and Wang, Y.H. (2005), "Experimental research on pre-cracked marble under compression", *J. Solids Struct.*, **42**(9-10), 2505-2516.
- Li, Y.Y., Zhou, H., Zhang L., Zhu, W., Li, S. and Liu, J. (2016), "Experimental and numerical investigations on mechanical property and reinforcement effect of bolted jointed rock mass", *Construct. Build. Mater.*, **126**, 843-856.
- Liu, X., Nie, Z., Wu, S. and Wang, C. (2015), "Self-monitoring application of conductive asphalt concrete under indirect tensile deformation", *Case Stud. Construct. Mater.*, **3**, 70-77.
- Mughieda, O. and Alzo'ubi, A.K. (2004), "Fracture mechanisms of offset rock joints-A laboratory investigation", *Geotech. Geol. Eng.*, **22**(4), 545-562.
- Mughieda, O. and Karasneh, I. (2006), "Coalescence of offset rock joints under biaxial loading", *Geotech. Geol. Eng.*, **24**(4), 985.
- Naghadehi, M.Z., Jimenez, R., KhaloKakaie, R. and Jalali, S.M.E. (2011), "A probabilistic systems methodology to analyze the importance of factors affecting the stability of rock slopes", *Eng. Geol.*, **118**(3-4), 82-92.
- Ning, J., Liu, X., Tan, Y., Wang, J. and Tian, C. (2015), "Relationship of box counting of fractured rock mass with Hoek-Brown parameters using particle flow simulation", *Geomech. Eng.*, **9**(5), 619-629.
- Noël, M. and Soudki, K. (2014), "Estimation of the crack width and deformation of FRP-reinforced concrete flexural members with and without transverse shear reinforcement", *Eng. Struct.*, **59**, 393-398.
- Panaghi, K., Golshani, A. and Takemura, T. (2015), "Rock failure assessment based on crack density and anisotropy index variations during triaxial loading tests", *Geomech. Eng.*, **9**(6), 793-813.
- Regmi, A.D., Yoshida, K., Nagata, H., Pradhan, A.M.S., Pradhan, B. and Pourghasemi, H.R. (2013), "The relationship between geology and rock weathering on the rock instability along Mugling-Narayanghat road corridor, Central Nepal Himalaya", *Nat. Hazards*, **66**(2), 501-532.
- Robertson, A.M., (1970), *The Interpretation of Geological Factors for Use in Slope Theory, in Planning Open Pit Mines*, Johannesburg, South Africa, 55-71.
- Sagong, M. and Bobet, A. (2002), "Coalescence of multiple flaws in a rock-model material in uniaxial compression", *J. Rock Mech. Min. Sci.*, **39**(2), 229-241.
- Sharma, R.K., Mehta, B.S. and Jamwal, C.S. (2013), "Cut slope stability evaluation of NH 21 along Nalayan-Gambhrola section, Bilaspur district, Himachal Pradesh, India", *Nat. Hazards*, **66**(2), 249-270.
- Shen, B., Stephansson, O., Einstein, H.H. and Ghahreman, B. (1995), "Coalescence of fractures under shear stress experiments", *J. Geophys. Res. Solid Earth*, **100**(B4), 5975-5990.
- Silva, R.V., De Brito, J. and Dhir, R.K. (2015), "Tensile strength behaviour of recycled aggregate concrete", *Construct. Build. Mater.*, **83**, 108-118.
- Singh, T.N., Gulati, A., Dontha, L. and Bhardwaj, V. (2008), "Evaluating cut slope failure by numerical analysis-A case study", *Nat. Hazards*, **47**, 263-279.
- Stimpson, B., (1970), "Modeling materials for engineering rock mechanics", *J. Rock Mech. Min. Sci. Geomech. Abstr.*, **7**(1), 77-121.
- Tian, Y., Shi, S., Jia, K. and Hu, S. (2015), "Mechanical and dynamic properties of high strength concrete modified with lightweight aggregates presaturated polymer emulsion", *Construct. Build. Mater.*, **93**, 1151-1156.
- Wang, H., Li, Y., Li, S., Zhang, Q. and Liu, J. (2016), "An elastoplastic damage constitutive model for jointed rock mass with an application", *Geomech. Eng.*, **11**(1), 77-94.
- Wang, Q.Z., Feng, F., Ni, M. and Gou, X.P. (2011), "Measurement of mode I and mode II rock dynamic fracture toughness with cracked straight through flattened Brazilian disc impacted by split Hopkinson pressure bar", *Eng. Fract. Mech.*, **78**(12), 2455-2469.
- Wang, Q.Z., Gou, X.P. and Fan, H. (2012), "The minimum dimensionless stress intensity factor and its upper bound for CCNBD fracture toughness specimen analyzed with straight through crack assumption", *Eng. Fract. Mech.*, **82**, 1-8.
- Wang, T., Dai, J.G. and Zheng, J.J. (2015), "Multi-angle truss model for predicting the shear deformation of RC beams with low span-effective depth ratios", *Eng. Struct.*, **91**, 85-95.
- Wang, X., Zhu, Z., Wang, M., Ying, P., Zhou, L. and Dong, Y. (2017), "Study of rock dynamic fracture toughness by using VB-SCSC specimens under medium-low speed impacts", *Eng. Fract. Mech.*, **181**, 52-64.
- Yang, S.Q. (2015), "An experimental study on fracture coalescence characteristics of brittle sandstone specimens combined various flaws", *Geomech. Eng.*, **8**(4), 541-557.
- Zhao, C. (2015), "Analytical solutions for crack initiation on floor-strata interface during mining", *Geomech. Eng.*, **8**(2), 237-255.
- Zhao, W., Huang, R. and Yan, M. (2015), "Mechanical and fracture behavior of rock mass with parallel concentrated joints with different dip angle and number based on PFC simulation",

*Geomech. Eng.*, **8**(6), 757-767.

CC